Biogeography of microbial bile acid transformations along the murine gut

Solenne Marion[1], Lyne Desharnais[1], Nicolas Studer[2], Yuan Dong[2], Matheus D. Notter[2], Suresh Poudel[3], Laure Menin[4], Andrew Janowczyk[5], Robert L. Hettich[3], Siegfried Hapfelmeier[2], Rizlan Bernier-Latmani[1]

Author information:

[1]*Environmental Microbiology Laboratory, École Polytechnique Fédérale de Lausanne (EPFL), Lausanne, Switzerland*

[2]*Institute for Infectious Diseases, University of Bern, Bern, Switzerland*

[3]*Chemical Sciences Division, Oak Ridge National Laboratory, Oak Ridge, TN, United States*

[4]*Institute of Chemical Sciences and Engineering, École Polytechnique Fédérale de Lausanne (EPFL), Lausanne, Switzerland*

[5]*Bioinformatics Core Facility, Swiss Institute of Bioinformatics, Lausanne, Switzerland*

Corresponding author:

Rizlan Bernier-Latmani

EPFL ENAC IIE EML

CH A1 375 (Bâtiment CH)

Station 6

CH-1015 Lausanne

Switzerland

Phone: +41 21 693-5001

Fax: +41 21 69 36205

Email: rizlan.bernier-latmani@epfl.ch

Abbreviations

BA, bile acid; CA, cholic acid; CDCA, chenodeoxycholic acid; UDCA, ursodeoxycholic acid; MCA, muricholic acid; DCA, deoxycholic acid; LCA, lithocholic acid; MDCA, murideoxycholic acid; HCA, hyocholic acid; HDCA, hyodeoxycholic acid; TGR5, Takeda G-protein receptor 5; FXR, farnesoid X receptor; Fgf15, fibroblast growth factor 15; BSH, bile salt hydrolase; HSDH, hydroxysteroid dehydrogenase; SPF, specific pathogen-free; GF, germ-free; CDI, *Clostridioides difficile* infection

Abstract

Bile acids, synthesized from cholesterol by the liver, are chemically transformed along the intestinal tract by the gut microbiota and the products of these transformations signal through host receptors, impacting overall host health. These transformations include bile acid deconjugation, oxidation, and 7α-dehydroxylation. An understanding of the biogeography of bile acid transformations in the gut is critical because deconjugation is a prerequisite for 7α-dehydroxylation and because most gut microorganisms harbor bile acid transformation capacity. Here, we used a coupled metabolomic and metaproteomic approach to probe *in vivo* activity of the gut microbial community in a gnotobiotic mouse model. Results revealed the involvement of *Clostridium scindens* in 7α-dehydroxylation, of the genera *Muribaculum* and *Bacteroides* in deconjugation, and of six additional organisms in oxidation (the genera *Clostridium*, *Muribaculum*, *Bacteroides*, *Bifidobacterium, Acutalibacter* and *Akkermansia*). Furthermore, the bile acid profile in mice with a more complex microbiota, with a dysbiosed microbiota or with no microbiota was considered. For instance, conventional mice harbor a large diversity of bile acids, but treatment with an antibiotic such as clindamycin results in complete inhibition of 7α-dehydroxylation, underscoring the strong inhibition of organisms able to carry out this process by this compound. Finally, comparison of the hepatic bile acid pool size as a function of microbiota revealed that a reduced microbiota affects host signaling but not necessarily bile acid synthesis. In this study, bile acid transformations were mapped to the associated active microorganisms, offering a systematic characterization of the relationship between microbiota and bile acid composition.

Keywords

Bile acids and salts, Bile acids and salts/Biosynthesis, Microbial metabolome, Microbiome, Proteomics, Oligo-MM^{12}, Fgf15, Cyp7a1, Sult2a8, FXR

Introduction

The gut is a complex ecosystem hosting a wide diversity of microorganisms. The gut microbiome is sometimes referred to as the forgotten endocrine organ because of its profound influence on host physiology. Gut microbes convert dietary and other exogenous molecules into signaling metabolites to communicate with the host[1]. Bile acids (BAs) are one of these microbiota-derived signaling metabolites.

Primary bile acids are synthesized in the liver from cholesterol (dietary or endogenous). In the hepatocytes, they are conjugated to glycine or taurine and stored continuously in the gall bladder as the main component of bile. The human liver synthesizes only two primary bile acids: cholic acid (CA) and chenodeoxycholic acid (CDCA), while the rodent liver synthesizes five: CA, CDCA, two muricholic acids (αMCA and βMCA) and ursodeoxycholic acid (UDCA), the 7β epimer of CDCA[2]. After food intake, the presence of fat molecules in the duodenum stimulates the release of a hormone, cholecystokinin, which triggers the contraction of the gall bladder and the relaxation of the Oddi sphincter, leading to the release of bile into the small intestine[3]. Along the intestinal tract, primary bile acids undergo several chemical transformations that are catalyzed by gut microorganisms, leading to the formation of secondary bile acids. Thus, the activity of the gut microbiota increases the diversity of the bile acid pool. The microbial transformation of the bile acid pool is essential as it modifies their detergent properties (i.e., their cytotoxicity) and also their affinity for host bile acid receptors[2]. For instance, the secondary bile acids deoxycholic acid (DCA) and lithocholic acid (LCA), resulting from microbial 7α-dehydroxylation of CA and CDCA, have a higher affinity for the membrane receptor Takeda G-protein receptor 5 (TGR5) compared to the host liver-derived primary bile acids[4,5].

Gut microorganisms act on the side chain, the hydroxyl groups, as well as the cyclohexane rings in the bile acid structure. Thus, microbial bile acid transformations include deconjugation or hydrolysis (i.e., the removal of the taurine/glycine moiety on the side chain), oxidation and epimerization of hydroxyl groups (at the C3, C7, and C12 positions) and of the C5-hydrogen, reduction of ketone groups, dehydroxylation at C7 and C12[6], desulfation[7], esterification of hydroxyl groups[8], and the oxidation of a steroid ring to form unsaturated bile acids[9,10] (Figure 1). Recently, a new microbial bile acid transformation was identified in both humans and mice: reconjugation. After being deconjugated by bacteria carrying bile salt hydrolase (BSH), the unconjugated bile acid can be reconjugated by bacteria with amino acids such as tyrosine, phenylalanine, leucine forming tyrosocholic acid, phenylalanocholic acid, and leucocholic acid respectively[11].

The abundance and diversity of bacteria carrying out the various bile acid transformations vary enormously. Deconjugating bacteria, synthesizing BSH, are reported to be abundant in the gut and widespread across bacterial phyla[12,13]. Similarly, oxidation of the hydroxyl groups in bile acids is also a common activity in gut microorganisms and is catalyzed by hydroxysteroid dehydrogenases (HSDHs)[14]. In contrast, 7α-dehydroxylating bacteria are considered as rare organisms in the gut and so far, only belong to the order Clostridiales[15]. The 7α-dehydroxylation reaction is catalyzed by a series of proteins (Bai proteins) encoded by genes belonging to the *bai* operon[16]. However, deconjugation is a prerequisite for bile acid 7α-dehydroxylation, thus the importance of considering the relative localization of these two bile acid transformations[17,18].

Connecting the spatial organization of the gut microorganisms to biological function remains challenging because of the high diversity of the gut microbial community[19]. For bile acid transformations, this difficulty is compounded by the large number of bile acid chemical species that can be generated by the gut microbiota. The original study of microbial bile acid transformation

biogeography dates back to 1968, when Midtvedt and Norman sampled luminal content along the intestinal tract of three rats and probed for *in vitro* bile acid transformations in each sample[20]. First, they noticed variability in the distribution of microbial bile acid transformations amongst the three rats. For instance, one rat had very little deconjugating activity in the small intestine (ileum) compared to the two other rats. Two rats showed 7α-HSDH activity (oxidation of the 7α-hydroxyl) in the ileum while the third rat did not. Since then, other studies have investigated bile acid profiles longitudinally[21,22]. However, probing for the presence/absence of specific bile acids may not accurately reflect the *in vivo* microbial bile acid transformation activity nor the presence/absence of the organisms responsible for the synthesis of that particular bile acid. For instance, it was recently observed that bile acid 7α-dehydroxylation activity was absent in the ileum of gnotobiotic mice despite colonization of the 7α-dehydroxylating organism, *Clostridium scindens*[23]. It was hypothesized that the high level of tauro-conjugated bile acids in the ileum likely precluded bile acid 7α-dehydroxylation[23]. Furthermore, the ability to transform bile acids *in vitro* does not necessarily reflect the *in vivo* activity. For instance, Narushima *et al.*, reported that the 7α-dehydroxylating bacterium *Clostridium hiranonis* (formerly *Clostridium strain* TO-931), known to deconjugate TCA to CA and to 7α-dehydroxylate cholic acid *in vitro* did not show any activity when amended to germ-free mice[24]. Thus, *in vivo* studies are needed to identify organisms active in bile acid metabolism within the microbial community of the gut.

In this study, we explored the longitudinal distribution of bile acid transformations in gnotobiotic mouse models and identified the microorganisms responsible for these transformations using a combined metabolomic and metaproteomic approach. Bile acid 7α-dehydroxylation was a transformation of particular interest because of its connection to TGR5 signaling. We contrasted gnotobiotic mice lacking bile acid 7α-dehydroxylating activity with gnotobiotic mice containing the same base microbiota but complemented with the 7α-dehydroxylating organism *Clostridium scindens* ATCC 35704. Finally, for comparison, we considered the bile acid profile in mice with

either a complex microbiota (conventional, specific pathogen-free (SPF) mice), a reduced microbiota (antibiotic-treated SPF mice), or no microbiota (germ-free).

Material and Methods

Animal experiments

Groups of age-matched C57BL/6 mice (6–12 weeks old) were used. Germ-free (GF) and gnotobiotic sDMDMm2 mice were established and maintained at the Clean Mouse Facility of the Department of Clinical Research of the University of Bern. sDMDMm2 mice were colonized with a mouse-intestine derived 12-species mouse microbiota (Oligo-MM^{12}) (Table S1)[25]. All Oligo-MM^{12} strains are available at http://www.dsmz.de/miBC. In-depth description of the Oligo-MM^{12} consortium species and description of novel taxa are provided elsewhere[26–28]. SPF mice were purchased from Envigo (formerly Harlan) and acclimatized to the local animal facility for 7 days before the start of experiments. SPF mice were pretreated with the antibiotic clindamycin (100µL by intra-peritoneal injection, 2 mg/mL in PBS) or streptomycin (100 µL by gavage, 200 mg/mL in PBS) 24h before sacrifice. sDMDMm2 mice were inoculated with *C. scindens* ATCC 35704 by gavage of 10^{7-9} CFU of *C. scindens* and colonized for 7 days before sacrifice. *C. scindens* pre-colonization was performed in flexible film isolators. These mice are denoted sDMDMm2+Cs.

All animals were sacrificed inside a sterile laminar flow hood and aseptic technique was used to collect the specific tissues and contents (liver, terminal ileum tissue, distal duodenum content, ileum content, cecum content and colon content). The collected samples were flash-frozen in liquid nitrogen and kept at -80°C to await subsequent analyses. All animal experiments were performed in accordance with the Swiss Federal and the Bernese Cantonal regulations and were approved by the Bernese Cantonal ethical committee for animal experiments under the license numbers BE 82/13 and BE111/16.

Quantitative Real-Time PCR

Liver (30 mg of the caudate lobe) and terminal ileum tissue were lysed and homogenized in tubes filled with 2.8 mm zirconium oxide beads using Precellys 24 Tissue Homogenizer (Bertin Instruments) at 6,500 rpm for 3x10 sec. Total RNA was isolated with the RNeasy Plus Mini Kit (QIAGEN). QuantiTect Reverse Transcription Kit (QIAGEN) was used to synthesized 20 µL cDNA templates from 1 µg of purified RNA. cDNA templates were diluted 10x before use in subsequent reactions. SensiFAST SYBR No-ROX Kit (Bioline) was used for quantitative real-time PCR with a final reaction volume of 10 µL (7.5 µL of mix and 2.5 µL of diluted cDNA template). Gene-specific primers (400nM) were used in each reaction and all results were normalized to the ribosomal protein L32 mRNA (primers sequences can be found in Table S2). PCR product specificity was verified by performance of a melting curve for each primer set. Assays were performed using Mic qPCR Cycler (Bio Molecular Systems) with a three-step program (2 min 95°C, followed by 40 cycles of 95°C for 5 s, 60°C for 10 s and 72 °C for 10 s). Four replicates of each sample for each primer set were performed, as well as negative controls (no reverse transcription and no template controls). Relative Quantification analysis using the REST method was performed with the Mic qPCR analysis software (Bio Molecular Systems).

Preparation of Bile Acid Standard Solutions

Stock solutions (10 mM) of each BA standard were prepared in methanol (Table S3). Individual standard solutions (100 µM) were mixed together and diluted with a 50:50 (v/v) mix of ammonium acetate (5 mM) and methanol to construct external standard curves between 1 and 10,000 nM. Deuterated CDCA and DCA were used as recovery standards.

Bile acid extraction

Approximately 10 mg of freeze-dried intestinal sample was homogenized with 150 µL of H_2O and spiked with 40 µL of recovery standard (100 µM) in 2 mL tubes filled with 2.8 mm zirconium

oxide beads. Homogenization was performed using an automated Precellys 24 Tissue Homogenizer (Bertin Instruments) at 5,000 rpm for 20 s. Mixed samples were equilibrated on ice for 1 h. A volume of 500 µL of ice-cold alkaline acetonitrile (5% ammonia in acetonitrile) was added to the homogenates, which were then vigorously vortexed, and continuously shaken for 1 h at room temperature. The mixtures were centrifuged at 16,000 x g for 10 min and the supernatants collected. The pellets were extracted with another 500 µL of ice-cold alkaline acetonitrile. Supernatants from the two extractions steps were pooled and lyophilized in a rotational vacuum concentrator (Christ) before reconstitution in 100 µL of a 50:50 (v/v) mix of ammonium acetate [5 mM] and methanol at pH 6, and stored at −20°C. Supernatants were diluted according to the intestinal compartment (4,000-fold for the small intestine and liver samples and 100-fold for the cecum and colon samples) before LC-MS injection. The extraction recovery ratios ranged between 75 and 85%.

Ultra-High-Pressure Liquid Chromatography-High Resolution Mass Spectrometry Analyses.

Both qualitative and quantitative analyses were conducted on an Agilent 6530 Accurate-Mass Q-TOF LC/MS mass spectrometer coupled to an Agilent 1290 series UHPLC system (Agilent). The separation was achieved using a Zorbax Eclipse-Plus C18 column (2.1 × 100 mm, 1.8 µm; Agilent) heated at 50°C. A binary gradient system consisted of 5 mM ammonium acetate pH 6 in water as eluent A and acetonitrile as eluent B. The sample separation was carried out at 0.4 mL/min over a 22 min total run time using the following program: 0–5.5 min, isocratic 21.5% B; 5.5–6 min, 21.5–24.5% B; 6–10 min, 24.5–25% B; 10–10.5 min, 25–29% B; 10.5–14.5 min, isocratic 29% B; 14.5–15 min, 29–40% B; 15–18 min, 40–45% B; 18–20.5 min, 45–95% B, 20.5–22 min, isocratic 95%. The system was re-equilibrated to initial conditions for 3 min. The sample manager system temperature was maintained at 4°C and the injection volume was 5 µL. Mass spectrometer detection was operated in negative ionization mode using the Dual AJS Jet stream ESI Assembly. The QTOF instrument was operated in the 4 GHz high-resolution mode (typical resolution 17,000 (FWHM) at m/z 1000) in profile mode and calibrated in negative full scan mode using ESI-L solution (Agilent).

Internal calibration was performed during acquisition via continuous infusion of a reference mass solution [5 mM purine, 1 mM HP-921 (Agilent reference mass kit) in 95% MeOH acidified with 0.1% formic acid] and allowed to permanently achieve a mass accuracy better than 5 ppm. HR mass spectra were acquired over the range of m/z 300– 700 at an acquisition rate of three spectra/s. AJS settings were as follows: drying gas flow, 8 L/min; drying gas temperature, 300°C; nebulizer pressure, 35 psi; capillary voltage, 3500 V; nozzle voltage, 1000 V; fragmentor voltage, 175 V; skimmer voltage, 65 V; octopole 1 RF voltage, 750 V. Data was processed using the MassHunter Workstation (Agilent). According to this method, 36 bile acids (Table S3) were quantified by external calibration curves. Extracted ions chromatograms (EIC) were based on a retention time (RT) window of ±0.5 min with a mass- extraction-windows (MEW) of ±30 ppm centered on m/z_{theor} of each bile acid.

Bile acid-metabolizing enzyme database

Whole genomes for the 12 Oligo-MM[12] species[28] and *C. scindens* ATCC 35704[17] were obtained from the NCBI and EBI (Accession numbers available in Table S4). Sequences were processed by Prodigal[29] to produce the gene sequences forming the BLASTP search database. Reference protein sequences for BSH, 3α-HSDH, 3β-HSDH, 7α-HSDH, 7β-HSDH, 12α-HSDH proteins were obtained from NCBI via the accession numbers presented in Table S5. These sequences were subsequently blasted against the produced protein database. The top 5 matches, as identified by bit score were selected for manual review. The final sequences with the highest scores were selected and are presented in Table S6.

Metaproteome analysis

Proteins were extracted from small intestine, cecum and colon content samples of sDMDMm2 (n=3) and sDMDMm2+Cs mice (n=3) at the Oak Ridge National Laboratory (Oak Ridge, TN, United States). Protein extraction and digestion followed by LC-MS/MS analysis were performed

as described previously[30] with slight modifications. Briefly, intestinal content samples were suspended in SDS lysis buffer (4% SDS, 100 mM Tris-HCl, 10 mM dithiothreitol, pH 8.0) and subjected to bead-beating. The proteins were isolated by chloroform-methanol extraction and resuspended in 4% sodium deoxycholate (SDC) in 100 mM ammonium bicarbonate (ABC) buffer. The crude protein concentration was estimated using a Nanodrop (Thermo Fisher Scientific). Protein samples (250 µg) were then transferred to a 10 kDa MWCO spin filter (Vivaspin 500, Sartorius), washed with ABC buffer, and digested with sequencing-grade trypsin.

After proteolytic digestion, the tryptic peptide solution was adjusted to 1% formic acid to precipitate the remaining SDC. The precipitated SDC was removed using water-saturated ethyl acetate. For each sample, 9 µg of peptides were analyzed by automated 2D LC-MS/MS using a Vanquish UHPLC with autosampler plumbed directly in-line with a Q Exactive Plus mass spectrometer (Thermo Fisher Scientific) across three successive salt cuts of ammonium acetate (35, 100 and 500 mM), each followed by a 155-minute organic gradient. Eluting peptides were measured and sequenced by data-dependent acquisition on the Q Exactive Plus as described earlier[31].

Peptide identification and protein inference were performed as follows: MS raw data files were searched against the protein database of 12 bacterial species genomes published by Garzetti *et al.* (2017)[28] and the *C. scindens* ATCC 35704 genome published by Devendran *et al.* (2019)[17] (Table S4) along with common contaminates (e.g., trypsin, human keratin) appended with a decoy database consisting of reverse protein sequences to control the false-discovery rate (FDR) to 1% at the spectral level[32].

MS/MS spectra data analysis (searching and filtering) was done by Crux mass spectrometry analysis toolkit (Crux version: 3.2-f7929ba)[33]. Tide-search[34] was used for searching. For Tide-search, default settings were used except for the following parameters: allowed clip n-term

methionine, allowed 4 missed-cleavages, a precursor mass tolerance of 10 parts per million (ppm), a static modification on cysteines (iodoacetamide; +57.0214 Da), dynamic modifications on methionine (oxidation; +15.9949), and a fragment ion mass tolerance of 0.02 Da. Trypsin was used as the digestion enzyme that cleaves C-terminal to arginine and lysine residues with an exception of proline in C-terminal to lysine and arginine. The obtained search result was processed by Percolator[35] to estimate q values using default parameters. MS1-level precursor intensities were derived from moFF[36] using default parameters along with match between runs features from biological replicates. An FDR cutoff of 1% was used as the peptide level. Protein intensities were calculated by summing together FDR-filtered quantified peptides, and normalized by performing LOESS and median central tendency procedures on log2-transformed values by InfernoRDN[37]. All proteins that had at least one unique peptide sequence were retained for biological interpretation. The list of proteins obtained along with their intensities is available in Supplemental Table S7.

All raw mass spectra for the proteome measurements have been deposited into the ProteomeXchange repository with the following accession numbers: (MassIVE Accession: MSV000084484, ProteomeXchange: PXD015971, FTP link to files: ftp://MSV000084484@massive.ucsd.edu, username: MSV000084484, Reviewer password: 'abcd1234')

Results and Discussion

Mapping bile acid transformations in gnotobiotic mice

The first goal of this study was to explore, using a combined metabolomic and metaproteomic approach, the longitudinal distribution of bile acid transformations in gnotobiotic mouse models (sDMDMm2 and sDMDMm2 + *C. scindens*) and to identify the microorganisms responsible for these transformations.

a) Bile salt deconjugation is an active transformation in the large intestine

Bile salt deconjugation (hydrolysis) constitutes the first step in the microbial bile acid metabolism (Figure 1)[13]. For instance, 7α-dehydroxylation requires unconjugated bile acids[18], while other processes such as dehydrogenation (oxidation) have been reported to occur with conjugated bile acid[14,38].

In the small intestine, the amendment of *C. scindens* to the Oligo-MM[12] microbial community led to a decrease in the deconjugating activity. Indeed, in the jejunum of *C. scindens*-colonized gnotobiotic mice, not only was the concentration of the dominant unconjugated primary BA (βMCA) 8-fold lower as compared to that in the sDMDMm2 cohort in absolute terms, but also, the ratio of βMCA to its conjugated counterpart (TβMCA) was 16-fold lower than in the microbiota lacking *C. scindens* (Figure 2). Accordingly, bile salt hydrolase (BSH) peptides were not detected in the small intestine of *C. scindens*-colonized gnotobiotic mice (Figure 3). In contrast, BSH expression was detected in all compartments in the sDMDMm2 cohort. Together, the bile acid profile and the BSH protein expression data suggest decreased BSH activity in the small intestine in the presence of *C. scindens* (Figures 2 and 3). This could be due either to differences in microbiota colonization of the gut or, more directly, to changes in the expression of the BSH enzymes. Notable differences are observed in the protein abundance of some strains in the small

intestine between the two gnotobiotic mouse models (e.g., *Blautia coccoides* YL58 and *Clostridium clostridioforme* YL32, Figure 4). However, protein abundance of the small intestine BSH-producer *M. intestinale YL27* is comparable between *C. scindens*-colonized mice and the control group (sDMDMm2 mice) (Figure 4). Thus, we hypothesize that expression of BSH enzymes is diminished in the *C. scindens*-colonized mice relative to the control.

In the large intestine of the two gnotobiotic mouse models, deconjugated bile acids predominate and BSH are detected, suggesting active bile salt hydrolysis in this compartment (Figures 2 and 3). In contrast to the small intestine, the protein abundance composition is comparable between the two gnotobiotic mouse models in the cecum and colon for all 12 strains (Figure 4).

While seven of the twelve organisms in the Oligo-MM[12] microbiota harbor BSH-encoding genes (Table S6), BSHs from only two organisms, *Muribaculum intestinale YL27* and *Bacteroides caecimuris I48,* were detected in the metaproteome (Figure 3 and Table S8). Thus, we propose that these two organisms are the main bile salt hydrolyzing strains in this mouse model. The BSH of *M. intestinale YL27* is highly expressed along the entire intestinal tract of sDMDMm2 animals, while the BSH of *B. caecimuris I48* was detectable only in the colon in both types of gnotobiotic mice (Figure 3).

Thus, based on the bile acid profile and the metaproteomic data of gnotobiotic mice (both sDMDMm2 and *C. scindens*-colonized sDMDMm2), we show that bile salt hydrolysis activity is mainly extant in the large intestine (Figures 2 and 3).

b) Bile acid oxidation is the most widespread transformation in the intestinal tract

Another common microbial bile acid transformation is oxidation (dehydrogenation), producing bile acids such as 3-oxoCA or 7-oxoDCA (Figure 1). There are several hypotheses regarding the role of bile acid oxidation. First, it increases the hydrophilicity of the bile acid pool, and consequently

reduces its toxicity for the host and the microbiota[39]. Thus, it could be considered a detoxification process. Second, it is also hypothesized that oxo- groups could serve as electron sinks[14]. Reduction of these oxo- groups would result in a net consumption of two electrons which would be favorable for fermenting bacteria in the anoxic environment of the large intestine, which is lacking in electrons acceptors[40].

Hydroxysteroid dehydrogenases (HSDH) catalyze the oxidation and epimerization of hydroxyl groups in the bile acid structure (Figure 1). Thirty-two predicted HSDHs were found in the genomes of the Oligo-MM[12] species and *C. scindens*. They include 3α-HSDH (oxidation of 3α-OH and reduction of 3-oxo group), 3β-HSDH (oxidation of 3β–OH and reduction of 3-oxo group), 7α-HSDH (oxidation of 7α-OH and reduction of 7-oxo group), 7β-HSDH (oxidation of 7β–OH and reduction of 7-oxo group) and 12α-HSDH (oxidation of 12α-OH and reduction of 12-oxo group) (Figure 1 and Table S6). Only 9 out of 32 predicted HSDHs were detected with the metaproteomic analysis (Figure 3, Tables S6 and S8) and corresponded exclusively to 3α-HSDH, 7α-HSDH, and 7β-HSDH (thus missing 3β-HSDH and 12α-HSDH). Furthermore, the bile acid profiles of gnotobiotic mice suggest that microbial oxidation of BAs only takes place in the large intestine (Figure 2).

Indeed, oxo- bile acids were not detected in the small intestine (Figure 2) despite the presence of 7β-HSDH from *C. innocuum I46* in sDMDMm2 mice and of 3α-HSDH from *B. caecimuris I48* in *C. scindens*-colonized sDMDMm2 mice (Figure 3, Table S8). We could speculate that the oxygen gradient[41] along the intestinal tract may have impacted the activity of the HSDH *in vivo,* but further research should be carried out to test this hypothesis. Hirano and Masuda (1981) reported that oxygen inhibited the activity of the 7α-HSDH of *Eubacterium lentum* (currently known as *Eggerthella lenta*)[42]. Thus, if the *C. innocuum* 7α-HSDH is oxygen-sensitive, the higher oxygen

level in the small intestine might inactivate its activity, precluding the formation of 7-oxo bile acids. However, oxygen sensitivity has never been reported for 3α-HSDH.

The metaproteomic analysis revealed that 7 species of the Oligo-MM[12] as well as *C. scindens* were producers of 3α-HSDH and/or 7α/β-HSDH in the intestinal tract of the gnotobiotic mice (Figure 3, Table S8).

Interestingly, the amendment of *C. scindens* clearly decreased the expression of 3α-HSDH *in vivo*. In the original gnotobiotic mice, 3α-HSDH from *Acutalibacter muris KB18*, *Akkermansia muciniphila YL44* and *B. caecimuris I48* were present in the large intestine, while in the mice amended with *C. scindens,* only the one from *B. caecimuris I48* was detected (Figure 3).

In contrast, the amendment of *C. scindens* enhanced the expression of 7α/β-HSDHs. The 7β-HSDH from *Bifidobacterium animalis YL2* and the 7α-HSDH from *C. scindens* were observed only in the metaproteome of *C. scindens*-colonized animals. Additionally, in both cohorts, the 7α-HSDHs from *M. intestinale YL27* and *B. caecimuris I48,* as well as the 7β-HSDH from *C. clostridioforme YL32* were encountered. These findings demonstrate that a single strain can profoundly alter the bile acid composition and expression of bile acid-metabolizing enzymes within a given microbial community. The remaining question is whether *C. scindens* affected the expression of enzymes directly or impacted the abundance of certain species. Previously, Studer *et al.* (2016) observed only minor changes in the fecal Oligo-MM[12] microbiota composition following the addition of *C. scindens*[43]. These minor changes included a decrease in abundance of *A. muris KB18* that could explain the absence of 3α-HSDH from this species in *C. scindens*-colonized cohort (Figure 3). However, the protein abundance for the 12 Oligo-MM[12] species is comparable in the large intestine of the two gnotobiotic mouse model, suggesting that the amendment of *C. scindens* has little impact on the large intestine microbial community (Figure 4).

Furthermore, Devendran and colleagues (2019) reported a downregulation, by the secondary bile acid DCA, of many genes encoding bile acid-transforming enzymes in *C. scindens*[17]. Amongst

them, *baiA2* (HDCHBGLK_01433) encodes a 3α-HSDH[44]. We hypothesize that *C. scindens*-specific metabolites, such as 7-dehydroxylated secondary bile acids (e.g., DCA), may affect the expression of bile acid-metabolizing enzymes by other bacteria of the Oligo-MM[12] consortium. The non-detection of 3α-HSDH associated with *A. muris KB18* and *A. muciniphila YL44* in gnotobiotic mice colonized with *C. scindens* (Figure 3) supports this hypothesis. Interestingly, 3β-HSDH were entirely absent in the metaproteome. Consistent with this result, iso- bile acids were not detected in the gnotobiotic animals (Figures 1 and 2). 12α-HSDH were also lacking in the metaproteome despite the presence of 12-oxoLCA in *C. scindens*-colonized mice (Figure 2). *C. scindens* is known to carry a gene encoding a 12α-HSDH and could be an active producer of 12-oxoLCA *in vivo*. Marion *et al*., (2018) reported the formation of 12-oxoLCA *in vitro* and proposed it as a transient intermediate of CA 7α-dehydroxylation by *C. scindens*[23]. Here, we hypothesize that 12α-HSDH from *C. scindens* is present in too low an abundance to be detected with metaproteomic analysis. In line with this hypothesis, the other enzymes of the 7α-dehydroxylation pathway were absent in the metaproteome despite the clear presence of 7α-dehydroxylated secondary bile acids (Figure 2).

c) Bile acid 7 α-dehydroxylation is restricted to the large intestine

The bile profile in the large intestine is very similar for mice models with and without *C. scindens*, with the exception of the presence of 7α-dehydroxylated species in the model including *C. scindens* (Figure 2). The 7α-dehydroxylated species detected include LCA, DCA and MDCA (murideoxycholic acid), the conjugated form of the latter two (TDCA and TMDCA), as well as 7α-dehydroxylated and oxidized species (6-oxoLCA, 6-oxo-alloLCA, 12-oxoLCA).

JOURNAL OF LIPID RESEARCH ASBMB

Amongst enzymes of the 7α-dehydroxylation pathway, only the 7α-hydroxy-3-oxo-Δ^4-cholenoic acid oxidoreductase (BaiCD)[45] was detected in the colon of *C. scindens*-colonized cohort. None of the Bai enzymes were detected in the small intestine samples of these mice (Figure 3, Table S8). Based on the metaproteomic and metabolomic data, we show that bile acid 7α-dehydroxylation occurs only in the large intestine of mice colonized with *C. scindens* (Figures 2 and 3). This observation supports an earlier study in which the large intestine was demonstrated to be the ecological niche of *C. scindens* in the gnotobiotic sDMDMm2 mouse model[23].

While all 12 microorganisms within the Oligo-MM[12] microbiota harbor bile acid-modifying enzymes (Table S6), peptides from only 7 of them were detected that mapped onto bile acid-related enzymes (Figure 3, Table S8). Because the metaproteomic approach is limited in measurement dynamic range, we cannot rule out the activity of the 5 other strains but can conclude that these 7 are the most active in bile acid transformations.

The second goal of the study was to assess the impact of the microbiota on the bile acid pool. To tackle this, we compared the bile acid pools of gnotobiotic mice to ones of mouse models with various gut microbiota complexities: a very complex microbiota (SPF), a reduced microbiota (antibiotic-treated SPF), or the absence of microbiota (germ-free).

The microbiota shapes the bile acid pool composition

Germ-free mice are devoid of microbial bile acid transformations. Thus, their bile acid pool is exclusively composed of liver-derived tauro-conjugated primary bile acids (Figures 5 and S2). TCA and TβMCA dominate the bile acid pool in all compartments (i.e., they represent ≈94% of the liver BA pool). Smaller contributions from TCDCA, TUDCA and TαMCA are also observed. In the

liver, a small fraction of unconjugated βMCA (836±544 nmol/g of tissue) is also noted along with very minor contributions (<10nmol/g of content) of the αMCA and βMCA in some intestinal compartments (ileum, cecum and colon). These observations support an earlier study from Sayin *et al* (2013)[21] who also observed minor fractions of unconjugated MCAs in germ-free mice. We hypothesize that the high bile acid synthesis activity in the liver does not allow for conjugating enzymes to act on all of the newly synthesized BA, resulting in the release into the intestine of a fraction of primary bile acids that have escaped conjugation in the liver. As expected, secondary bile acids are altogether absent in the GF mouse intestine due to the dearth of microorganisms.

For comparison, we also considered SPF animals with or without antibiotic treatment. As expected, SPF mice exhibited the highest bile acid diversity (Figure 5). Secondary bile acids in SPF mice are present in the small intestine, while in *C. scindens*-bearing gnotobiotic animals, they were detected only in the large intestine (Figures 2 and 5). As the mouse liver is able to re-conjugate deconjugated BA, tauro-conjugated 7α-dehydroxylated bile acids (TMDCA, THDCA, TDCA, TωMCA) are observed in the upper intestinal tract. Thus, it is not possible to determine whether the 7α-dehydroxylated bile acids DCA and HDCA in the small intestine come from 7α-dehydroxylation of CA and HCA (the 6α epimer of αMCA) or from the deconjugation of TDCA and THDCA in that compartment (Figure 5).

In contrast to the other models, secondary bile acids represent more than half of the bile acid pool in the large intestine of SPF mice and the conjugated bile acids are present at low levels (Figure S2). Additionally, 7α-dehydroxylated secondary bile acids, comprising the 7-dehydroxylated form of the primary bile acids (DCA, LCA, MDCA, HDCA), the oxidized species (12oxoLCA, 3-oxoLCA, 6-oxoLCA, 6-oxo-alloLCA) and the epimerized species (isoLCA, alloLCA), represent 57% of the pool of secondary BA (Figures 5 and S2). Finally, SPF mice are the only mice to

produce iso-bile acid (3β-epimers), allo-bile acids (5α-epimers), and 6β-epimers (e.g., HCA) in the large intestine (Figure 5).

Antibiotic treatment had a tremendous impact on bile acid transformation throughout the intestinal tract. In the small intestine, bile acid diversity was extremely reduced compared to that in untreated SPF mice (Figure 5). The most salient impacts are the suppression of bile acid deconjugation in the small intestine and the complete abolition of 7α-dehydroxylation by the clindamycin treatment (Figure 5). Streptomycin-treated animals exhibited decreased amounts of 7α-dehydroxylated species but this antibiotic was not as efficient as clindamycin at inhibiting 7α-dehydroxylation, suggesting the survival of 7α-dehydroxylating bacteria to streptomycin treatment (Figure S1). Interestingly, tauroconjugated 7α-dehydroxylated species (TMDCA and THDCA) were detected in the small intestine (Figure 5). We attribute the presence of those species to the 7-dehydroxylation of MCAs (α-, β-, ω-MCA) and HCA prior to the antibiotic treatment, followed by recycling via the enterohepatic circulation and reconjugation in the liver before release into the small intestine.

7α-dehydroxylated bile acids have been linked to protection against *Clostridioides difficile* infections (CDI) through the inhibitory role of 7-dehydroxylated BAs in *C. difficile* spore germination and outgrowth[46,47]. Based on the bile acid profile of clindamycin- and streptomycin-treated mice (Figures 5 and S1), it would be predicted that treatment with streptomycin is less of a risk factor for CDI as compared to that with clindamycin, and that 7α-dehydroxylating organisms are sensitive to clindamycin but not streptomycin. In accordance with these hypothesis, Theriot *et al.* (2016) showed that cecal content from mice treated with clindamycin triggers spore germination and cells outgrowth of *C. difficile*[48].

Furthermore, Slimings and Riley (2014) reported no association between the use of aminoglycosides (an antibiotic class that includes streptomycin) and CDI, while clindamycin was the antibiotic most frequently associated with CDI (both hospital-acquired and community-

acquired) in patient meta-analyses[49–51]. Additionally, two of the major bile acid 7α-dehydroxylating organisms, *C. scindens* and *C. hylemonae,* are sensitive to clindamycin (Table S9). Furthermore, two studies observed that restricting the use of clindamycin led to a sustained decrease in CDI[52,53]. Buffie *et al*. (2015), observed that the cecal microbiota of SPF mice treated with clindamycin underwent profound losses of *Lachnospiraceae,* a family that includes several 7α-dehydroxylating strains (e.g., *C. scindens* and *C. hylemonae*)[54]. These observations are all consistent with clindamycin effectively inhibiting BA 7-dehydroxylation and thus, creating conditions propitious for the germination and outgrowth of *C. difficile* spores. These data support previous research that reported drastic changes in the fecal BA pool following antibiotic treatment[48,55]. The novelty of the present study is the extensive bile acid profile for the liver and four intestinal compartments (duodenum, ileum, cecum and colon). Other studies have focused on fewer sample type (liver and plasma samples[55], or gallbladder and serum[21], or ileum and cecum[48]). Furthermore, the number of bile acids screened in this study is greater compared to previous studies[21,48,55], offering more in-depth reporting of the impact of antibiotic treatment on bile acid composition. This study also reports for the first time the antibiotic susceptibility profiles of three major bile acid 7-dehydroxylating species *C. scindens*, *C. hylemonae* and *C. hiranonis* (Table S9).

Microbiota-host interactions regulate the bile acid pool size

Supporting earlier research[21], our data show that germ-free mice harbor an abundant bile acid pool (Figures 5 and S2). Here, we also observed that mouse models with a reduced microbiota (gnotobiotic and antibiotic-treated mice) have an increased hepatic bile acid pool compared to conventional mice (SPF) harboring a more diverse microbiota (Figure 6a). Furthermore, we noted a large inter-individual variability of the hepatic BA pool in GF and gnotobiotic mice cohorts compared to that in SPF and antibiotic-treated SPF mice (Figure 6a). This clearly indicates that BA synthesis is more tightly regulated in hosts with more complex microbial communities (e.g., SPF).

In mammals, the nuclear receptor farnesoid X receptor (FXR), highly expressed in the ileum[56], controls hepatic bile acid synthesis through a negative feedback loop[57]. The activation of FXR by bile acids induces the release of fibroblast growth factor 15 (Fgf15) in the intestine, which reaches the liver via portal vein circulation and inhibits the expression of the hepatic enzyme Cyp7a1 (cholesterol 7α-hydroxylase), responsible for catalyzing the rate-limiting step in bile acid synthesis[21].

The tauro-conjugated murine primary BAs are strong antagonists of FXR[58], while CDCA, and the 7α-dehydroxylated species DCA and LCA are potent FXR agonists[59], thus acting as repressors of bile acid synthesis. Gut microbes are important actors in FXR-mediated regulation of bile acid synthesis because they decrease the concentration of FXR antagonists (e.g., TβMCA, TαMCA) and produce unconjugated bile acids and secondary bile acids, which activate FXR[21]. The role of the deconjugating microbial community is particularly important as deconjugation contributes to a decrease in the concentration of the FXR antagonists TMCAs[60] and allows further transformation such as 7α-dehydroxylation[18]. Germ-free mice, devoid of microbial bile acid transformations, have the largest bile acid pool size compared to that of other mice models harboring a microbial community (Figures 5 and S2). As previously demonstrated[21], we observed that the concentration of TβMCA was high in germ-free mice, resulting from the absence of microbial deconjugation (Figure 5). Consequently, the FXR-dependent negative feedback loop was inhibited, resulting in increased bile acid synthesis[21] and hepatic bile acid pool (Figure 6a).

The ileal ratio of FXR antagonists (TMCAs) over FXR agonists[59] (CDCA+CA+TCDCA+TCA+DCA+LCA+TDCA+TLCA) is a good indicator of the size of the hepatic bile acid pool (Figure 6b). Indeed, this relationship offers an explanation as to why *C. scindens*-colonized sDMDMm2 mice have a higher bile acid pool size compared to sDMDMm2 mice (Figure 6a). This higher pool size is due to the increased FXR antagonist/agonist ratio in those

mice relative to mice lacking *C. scindens* (Figure 6b), explaining the higher bile acid synthesis. The increased ratio is likely due to reduced BSH activity in the small intestine, as is reflected in the metaproteomic data, with no BSH activity detected in the small intestine (Figure 3). The reduced BSH activity leads to an increased concentration of FXR antagonists (particularly TMCAs) in the ileum. Indeed, TβMCA level is 3-fold greater in the ileum of *C. scindens*-colonized cohort compared to that in the sDMDMm2 animals (Figure 2). Similarly to the hepatic BA pool, there is a large inter-individual variability in the ileal FXR antagonist/agonist ratio in germ-free and gnotobiotic cohorts compared to that in SPF and antibiotic-treated SPF mice (Figure 6b). This ileal ratio is relevant only for mouse studies as it takes into account the murine specific conjugated primary BA (TMCA) as FXR antagonists, which are absent in humans. In humans, very little is known about endogenous FXR antagonists. Only LCA has been reported to have an FXR antagonist activity in addition to a partial agonist activity in cells[61]. Further research is needed to investigate the ligand potency of human primary, secondary and tertiary bile acids towards the FXR receptor.

Antibiotic treatment also affects BA deconjugating activity, and most likely, FXR signaling, leading to increased bile acid synthesis (Figure 6). In order to better understand the FXR-mediated regulation of bile acid synthesis by the gut microbiota, we measured the ileal expression of *Fgf15* and hepatic expression of *Cyp7a1* in our mice models. Mice models with no or a reduced microbiota (GF, gnotobiotic and antibiotic-treated SPF) show a significantly reduced ileal expression of *Fgf15* (more than 10-fold) relative to SPF mice (Figure 6e).

The expression of *Cyp7a1* is significantly increased in antibiotic-treated mice compared to untreated ones (Figure 6d). In contrast, we did not detect a significant difference in *Cyp7a1* expression between GF and SPF as previously reported by Sayin *et al*. (2013). However, the increase reported by Sayin *et al*. (2013) is only 2-fold and could be considered minor when discussing gene expression. In line with our observation, a recent thesis, reported no difference in

Cyp7a1 mRNA expression between GF and SPF with a chow diet[62]. Although not statistically significant, *C. scindens*-colonized mice show an increased *Cyp7a1* expression compared to sDMDMm2 and GF mice which is consistent to the higher bile acid pool (Figure 6d).

Altogether, these data show that having a reduced microbiota impacts FXR signalling (via the downregulation of *Fgf15*). Bile acid synthesis was mostly impacted by the antibiotic-mediated dysbiosis. There is a large inter-individual variation in the hepatic BA pool and ileal FXR antagonist / agonist ratio in germ-free and gnotobiotic mice (Figure 6a, b, c) which is not observed in SPF and antibiotic-treated mice. This suggest that the bile acid synthesis is more tightly regulated in mice harboring a more diverse microbial community.

Bile acid detoxification

Intestinal sulfated bile acids were measured in this study. Bile acid sulfation is a major host metabolic pathway to detoxify and eliminate bile acids. Sulfotransferases (e.g., Sult2a1) catalyze the sulfation (or sulfonation) of bile acids in the liver. Sulfation of BAs increases their solubility, reduces the intestinal absorption, and consequently fosters their urinary and fecal elimination. In humans, about 70% of the bile acid pool in the urine is sulfated but under pathological conditions (e.g., cholestatic diseases), the fraction of sulfated bile acid increases[63].

Sulfation in SPF mice is low compared to the germ-free, gnotobiotic and antibiotic-treated mouse models (Figures 2 and 5). In SPF mice, sulfated bile acids are not detected in the liver and the amount of sulfated BAs in the intestine are 2-fold smaller than those of the mouse models with a reduced microbial community (Figure 2 and 5). Miyata *et al.* (2006), reported that the hepatic sulfotransferase Sult2a1 is negatively regulated through FXR in mice and humans[64]. Sult2a8 was recently identified as a major bile acid sulfonating enzyme in mice[65]. Here, we observed that

expression of *Sult2a8* was comparable amongst the various mouse models, suggesting that Sult2a8 is not regulated through FXR nor influenced by the gut microbiota (Figure 6f).

Conclusion

Bile acids exert crucial functions in the host that go beyond their role as lipid detergents and gut microbes play a central role in the bile acid metabolism. By modifying the structure of the bile acid, microorganisms influence their affinity to host bile acid receptors. In this study, we characterized the biogeography of bile acid transformation in gnotobiotic mice. We identify the main organisms involved in bile acid metabolism in a gnotobiotic mouse model and the localization of their activity in the gut. Furthermore, by comparing the bile acid profiles of mouse models with either reduced or more complex microbiota, we emphasized the profound influence of the gut microbial community on the regulation of the bile acid pool size and composition. Finally, by measuring the expression of *Fgf15*, *Cyp7a1* and *Sult2a8*, we demonstrated that a reduced microbiota affects FXR signaling but not necessarily bile acid synthesis. The latter was mainly impacted by antibiotic-mediated dysbiosis. Finally, we report that bile acid sulfonation by Sult2a8, the major BA sulfotransferase in mice, does not seem to be FXR mediated, nor influenced by the gut microbiota.

Data availability

As indicated in the Material and Method section, all raw mass spectra for the proteome measurements have been deposited into the ProteomeXchange repository with the following accession numbers: (MassIVE Accession: MSV000084484, ProteomeXchange: PXD015971, FTP link to files: ftp://MSV000084484@massive.ucsd.edu, username: MSV000084484, Reviewer password: 'abcd1234'). All other data are either contained in the article or available upon request from the corresponding author.

Acknowledgements

This research was funded by the Swiss National Science Foundation (Sinergia grants #CRSII3_147603 and #CRSII5_180317). We thank Dr. Gilbert Greub and Dr. Guy Prod'Hom from the Microbiology Institute at CHUV for their help with the antimicrobial susceptibility testing. Mice were obtained from the Clean Mouse Facility (CMF) of the University of Bern, Switzerland. We thank the academic and technical staff of the CMF for their services and support. We thank Alessia Perino in the lab of Kristina Schoonjans at EPFL for her assistance with the qRT-PCR. We thank Léonard Jequier from the group of Mauro Delorenzi for his assistance with the bioinformatic analysis.

Conflict of Interest

The authors declare that they have no conflict of interest.

References

1. Schroeder, B. O. & Bäckhed, F. Signals from the gut microbiota to distant organs in physiology and disease. *Nature Medicine* vol. 22 1079–1089 (2016).
2. Wahlström, A., Sayin, S. I., Marschall, H. U. & Bäckhed, F. Intestinal Crosstalk between Bile Acids and Microbiota and Its Impact on Host Metabolism. *Cell Metabolism* vol. 24 41–50 (2016).
3. Hofmann, A. F. The continuing importance of bile acids in liver and intestinal disease. *Arch. Intern. Med.* **159**, 2647–2658 (1999).
4. Wahlström, A. *et al.* Intestinal Crosstalk between Bile Acids and Microbiota and Its Impact on Host Metabolism. *Cell Metab* **24**, 41–50 (2016).
5. Ridlon, J. J. M., Kang, D. J. D., Hylemon, P. B. P. & Bajaj, J. J. S. Bile acids and the gut microbiome. *Curr. Opin. Gastroenterol.* **30**, 332–8 (2014).
6. Edenharder, R. Dehydroxylation of cholic acid at C12 and epimerization at C5 and C7 by Bacteroides species. *J. Steroid Biochem.* **21**, 413–420 (1984).
7. Huijghebaert, S., Parmentier, G. & Eyssen, H. *Specificity of bile salt sulfatase activity in man, mouse and rat intestinal microflora*. *J. steroid Biochem* vol. 20 (1984).
8. Kelsey, M. I., Molina, J. E., Huang, S. K. & Hwang, K. K. The identification of microbial metabolites of sulfolithocholic acid. *J. Lipid Res.* **21**, 751–9 (1980).
9. Macdonald, I. A., Bokkenheuser, V. D., Winter, J., McLernon, A. M. & Mosbach, E. H. Degradation of steroids in the human gut. *J. Lipid Res.* **24**, 675–700 (1983).
10. Prabha, V. & Ohri, M. Review: Bacterial transformations of bile acids. *World J. Microbiol. Biotechnol.* **22**, 191–196 (2006).
11. Quinn, R. A. *et al.* Chemical Impacts of the Microbiome Across Scales Reveal Novel Conjugated Bile Acids. *bioRxiv* 654756 (2019) doi:10.1101/654756.
12. Urdaneta, V. *et al.* Interactions between Bacteria and Bile Salts in the Gastrointestinal and

Hepatobiliary Tracts. *Front. Med.* **4**, 163 (2017).

13. Foley Id, M. H., O'flaherty Id, S., Id, R. B. & Theriot Id, C. M. Bile salt hydrolases: Gatekeepers of bile acid metabolism and host-microbiome crosstalk in the gastrointestinal tract. (2019) doi:10.1371/journal.ppat.1007581.
14. Doden, H. *et al.* Metabolism of oxo-bile acids and characterization of recombinant 12α-hydroxysteroid dehydrogenases from bile acid 7α-dehydroxylating human gut bacteria Clostridium scindens ATCC 35704, Clostridium hylemonae DSM 15053 and Clostridium hiranonis DSM 13275. *Appl. Environ. Microbiol.* (2018) doi:10.1128/AEM.00235-18.
15. Ridlon, J. M., Kang, D. J. & Hylemon, P. B. Bile salt biotransformations by human intestinal bacteria. *J. Lipid Res.* **47**, 241–59 (2006).
16. Ridlon, J. M., Harris, S. C., Bhowmik, S., Kang, D.-J. J. & Hylemon, P. B. Consequences of bile salt biotransformations by intestinal bacteria. *Gut Microbes* **7**, 22–39 (2016).
17. Devendran, S. *et al.* Clostridium scindens ATCC 35704: Integration of nutritional requirements, the complete genome sequence, and global transcriptional responses to bile acids. *Appl. Environ. Microbiol.* **85**, (2019).
18. Batta, A. K. *et al.* Side chain conjugation prevents bacterial 7-dehydroxylation of bile acids. *J. Biol. Chem.* **265**, 10925–10928 (1990).
19. Tropini, C., Earle, K. A., Huang, K. C. & Sonnenburg, J. L. The Gut Microbiome: Connecting Spatial Organization to Function. *Cell Host Microbe* **21**, 433–442 (2017).
20. Midtvedt, T. & Norman, A. Anaerobic, bile acid transforming microorganisms in rat intestinal content. *Acta Pathol. Microbiol. Scand.* **72**, 337–344 (1968).
21. Sayin, S. I. *et al.* Gut microbiota regulates bile acid metabolism by reducing the levels of tauro-beta-muricholic acid, a naturally occurring FXR antagonist. *Cell Metab.* **17**, 225–235 (2013).
22. Selwyn, F. P., Csanaky, I. L., Zhang, Y. & Klaassen, C. D. Importance of large intestine in regulating bile acids and glucagon-like peptide-1 in germ-free mice. *Drug Metab. Dispos.*

43, 1544–1556 (2015).

23. Marion, S. *et al.* In vitro and in vivo characterization of Clostridium scindens bile acid transformations. *Gut Microbes* **10**, 481–503 (2018).

24. Narushima, S., Itoh, K., Takamine, F. & Uchida, K. Absence of cecal secondary bile acids in gnotobiotic mice associated with two human intestinal bacteria with the ability to dehydroxylate bile acids in vitro. *Microbiol. Immunol.* **43**, 893–897 (1999).

25. Eberl, C. *et al.* Reproducible Colonization of Germ-Free Mice With the Oligo-Mouse-Microbiota in Different Animal Facilities. *Front. Microbiol.* (2020) doi:10.3389/fmicb.2019.02999.

26. Lagkouvardos, I. *et al.* The Mouse Intestinal Bacterial Collection (miBC) provides host-specific insight into cultured diversity and functional potential of the gut microbiota. *Nat Microbiol* **1**, 16131 (2016).

27. Brugiroux, S. *et al.* Genome-guided design of a defined mouse microbiota that confers colonization resistance against Salmonella enterica serovar Typhimurium. *Nat Microbiol* **2**, 16215 (2016).

28. Garzetti, D. *et al.* High-Quality Whole-Genome Sequences of the Oligo-Mouse-Microbiota Bacterial Community. *Genome Announc.* **5**, e00758-17 (2017).

29. Hyatt, D. *et al.* Prodigal: prokaryotic gene recognition and translation initiation site identification. *BMC Bioinformatics* **11**, 119 (2010).

30. Patnode, M. L. *et al.* Interspecies Competition Impacts Targeted Manipulation of Human Gut Bacteria by Fiber-Derived Glycans. (2019) doi:10.1016/j.cell.2019.08.011.

31. Clarkson, S. M. *et al.* Construction and Optimization of a Heterologous Pathway for Protocatechuate Catabolism in Escherichia coli Enables Bioconversion of Model Aromatic Compounds. *Appl. Environ. Microbiol.* **83**, e01313-17 (2017).

32. Elias, J. E. & Gygi, S. P. Target-decoy search strategy for increased confidence in large-scale protein identifications by mass spectrometry. *Nat. Methods* **4**, 207–214 (2007).

33. Park, C. Y., Klammer, A. A., Käli, L., MacCoss, M. J. & Noble, W. S. Rapid and accurate peptide identification from tandem mass spectra. *J. Proteome Res.* (2008) doi:10.1021/pr800127y.

34. Diament, B. J. & Noble, W. S. Faster SEQUEST Searching for Peptide Identification from Tandem Mass Spectra. *J. Proteome Res.* **10**, 3871–3879 (2011).

35. Käll, L., Canterbury, J. D., Weston, J., Noble, W. S. & MacCoss, M. J. Semi-supervised learning for peptide identification from shotgun proteomics datasets. *Nat. Methods* **4**, 923–5 (2007).

36. Argentini, A. *et al.* moFF: a robust and automated approach to extract peptide ion intensities. *Nat. Methods* **13**, 964–966 (2016).

37. Polpitiya, A. D. *et al.* DAnTE: a statistical tool for quantitative analysis of -omics data. *Bioinformatics* **24**, 1556–8 (2008).

38. Harris, S. C. *et al.* Bile acid oxidation by Eggerthella lenta strains C592 and DSM 2243 T. *Gut Microbes* **9**, 523–539 (2018).

39. Watanabe, M., Fukiya, S. & Yokota, A. Comprehensive evaluation of the bactericidal activities of free bile acids in the large intestine of humans and rodents. *J. Lipid Res.* (2017) doi:10.1194/jlr.M075143.

40. Winter, S. E., Lopez, C. A. & Bäumler, A. J. The dynamics of gut-associated microbial communities during inflammation. *EMBO Reports* (2013) doi:10.1038/embor.2013.27.

41. Donaldson, G. P., Lee, S. M. & Mazmanian, S. K. Gut biogeography of the bacterial microbiota. *Nat. Rev. Microbiol.* **14**, 20–32 (2015).

42. Hirano, S. & Masuda, N. Transformation of bile acids by Eubacterium lentum. *Appl. Environ. Microbiol.* **42**, 912–5 (1981).

43. Studer, N. *et al.* Functional Intestinal Bile Acid 7α-Dehydroxylation by Clostridium scindens Associated with Protection from Clostridium difficile Infection in a Gnotobiotic Mouse Model. *Front. Cell. Infect. Microbiol.* **6**, 191 (2016).

44. Bhowmik, S. *et al.* Structural and functional characterization of BaiA, an enzyme involved in secondary bile acid synthesis in human gut microbe. *Proteins* **82**, 216–29 (2014).

45. Kang, D.-J. *et al.* Clostridium scindens baiCD and baiH genes encode stereo- specific 7α/7β-hydroxy-3-oxo-Δ 4 -cholenoic acid oxidoreductases. *Biochim Biophys Acta* **1781**, 16–25 (2008).

46. Shen, A. *et al.* A Gut Odyssey: The Impact of the Microbiota on Clostridium difficile Spore Formation and Germination. *PLoS Pathog.* **11**, (2015).

47. Buffie, C. G. *et al.* Precision microbiome reconstitution restores bile acid mediated resistance to Clostridium difficile. *Nature* **517**, 205–8 (2015).

48. Theriot, C. M., Bowman, A. A. & Young, V. B. Antibiotic-Induced Alterations of the Gut Microbiota Alter Secondary Bile Acid Production and Allow for Clostridium difficile Spore Germination and Outgrowth in the Large Intestine. *mSphere* **1**, (2016).

49. Deshpande, A. *et al.* Community-associated clostridium difficile infection antibiotics: A meta-analysis. *Journal of Antimicrobial Chemotherapy* vol. 68 1951–1961 (2013).

50. Brown, K. A., Khanafer, N., Daneman, N. & Fisman, D. N. Meta-analysis of antibiotics and the risk of community-associated Clostridium difficile infection. *Antimicrob. Agents Chemother.* **57**, 2326–2332 (2013).

51. Slimings, C. & Riley, T. V. Antibiotics and hospital-acquired Clostridium difficile infection: Update of systematic review and meta-analysis. *Journal of Antimicrobial Chemotherapy* vol. 69 881–891 (2014).

52. Pear, S. M., Williamson, T. H., Bettin, K. M., Gerding, D. N. & Galgiani, J. N. Decrease in nosocomial Clostridium difficile-associated diarrhea by restricting clindamycin use. *Ann. Intern. Med.* **120**, 272–7 (1994).

53. Climo, M. W. *et al.* Hospital-wide restriction of clindamycin: effect on the incidence of Clostridium difficile-associated diarrhea and cost. *Ann. Intern. Med.* **128**, 989–95 (1998).

54. Buffie, C. G. *et al.* Profound alterations of intestinal microbiota following a single dose of

clindamycin results in sustained susceptibility to Clostridium difficile-induced colitis. *Infect. Immun.* **80**, 62–73 (2012).

55. Swann, J. R. *et al.* Systemic gut microbial modulation of bile acid metabolism in host tissue compartments. *Proc. Natl. Acad. Sci.* **108**, 4523–4530 (2011).

56. Houten, S. M., Volle, D. H., Cummins, C. L., Mangelsdorf, D. J. & Auwerx, J. In Vivo Imaging of Farnesoid X Receptor Activity Reveals the Ileum as the Primary Bile Acid Signaling Tissue. *Mol. Endocrinol.* **21**, 1312–1323 (2007).

57. Chiang, J. Y. L. Bile acids: regulation of synthesis. *J. Lipid Res.* **50**, 1955–1966 (2009).

58. Wang, H., Chen, J., Hollister, K., Sowers, L. C. & Forman, B. M. Endogenous Bile Acids are Ligands for the Nuclear Receptor FXR/BAR. *Mol. Cell* **3**, 543–553 (1999).

59. Parks, D. J. *et al.* Bile acids: Natural ligands for an orphan nuclear receptor. *Science (80-.).* **284**, 1365–1368 (1999).

60. Li, F. *et al.* Microbiome remodelling leads to inhibition of intestinal farnesoid X receptor signalling and decreased obesity. *Nat. Commun.* **4**, 2384 (2013).

61. Yu, J. *et al.* Lithocholic acid decreases expression of bile salt export pump through farnesoid X receptor antagonist activity. *J. Biol. Chem.* (2002) doi:10.1074/jbc.M200474200.

62. Just, S. Impact of the interplay between bile acids , lipids , intestinal Coriobacteriaceae and diet on host metabolism. *These* (2017).

63. Alnouti, Y. Bile Acid Sulfation: A Pathway of Bile Acid Elimination and Detoxification. *Toxicol. Sci.* **108**, 225–246 (2009).

64. Miyata, M. *et al.* Chenodeoxycholic acid-mediated activation of the farnesoid X receptor negatively regulates hydroxysteroid sulfotransferase. *Drug Metab. Pharmacokinet.* **21**, 315–23 (2006).

65. Dawson, P. A. & Setchell, K. D. R. Will the real bile acid sulfotransferase please stand up? Identification of Sult2a8 as a major hepatic bile acid sulfonating enzyme in mice. *J.*

Lipid Res. (2017) doi:10.1194/jlr.C077420.

66. Huijghebaert, S. M., Mertens, J. A. & Eyssen, H. J. Isolation of a bile salt sulfatase-producing Clostridium strain from rat intestinal microflora. *Appl. Environ. Microbiol.* **43**, 185–92 (1982).

Figures

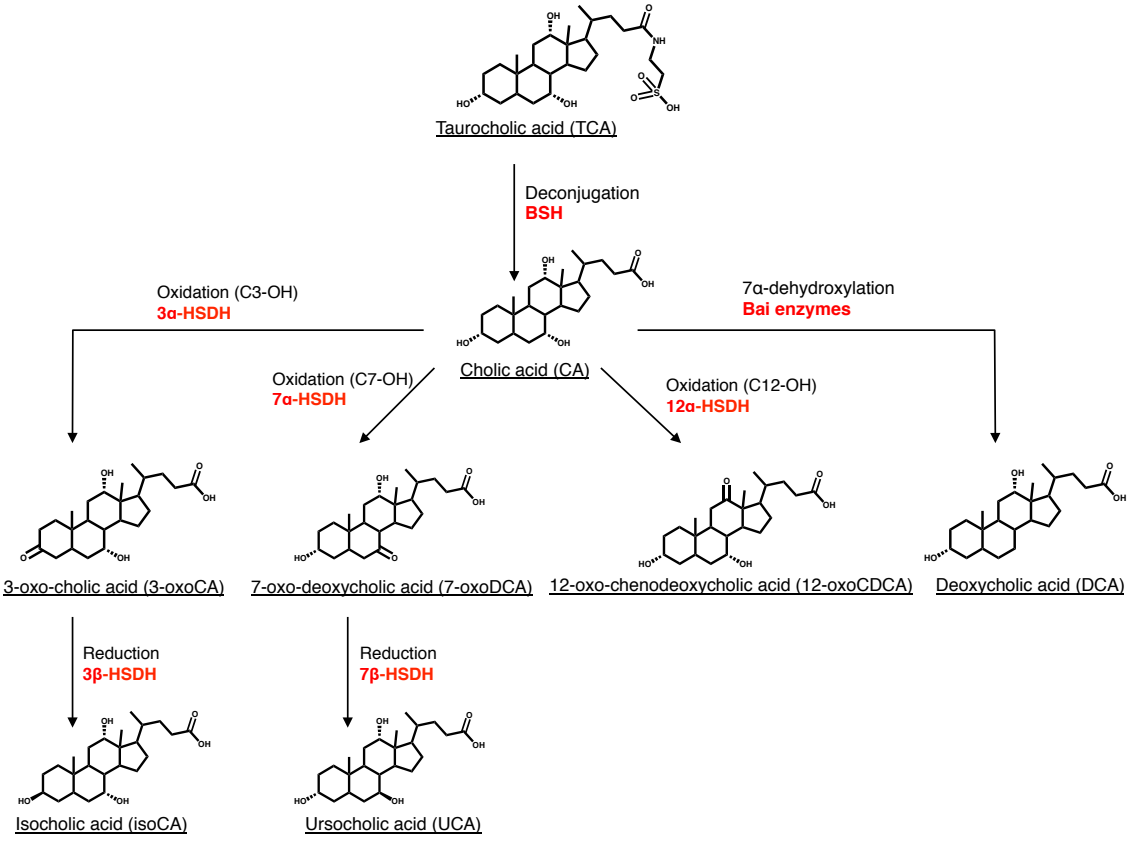

Figure 1 | Microbial bile acid transformations.

Deconjugation (bile salt hydrolysis), oxidation of hydroxyl groups, reduction of ketone group and bile acid 7α-dehydroxylation are major bile acid transformations occurring in the intestinal tract and are those on which we focused in this study. The enzymes catalyzing each transformation are indicated in red. Other microbial bile acid transformations (e.g., desulfation[66], reconjugation[11], the oxidation of C12-hydroxyl group on taurocholic acid by 12α-HSDH[14,38]) are not presented in this figure for the sake of clarity. BSH, bile salt hydrolase; HSDH, hydroxysteroid dehydrogenase.

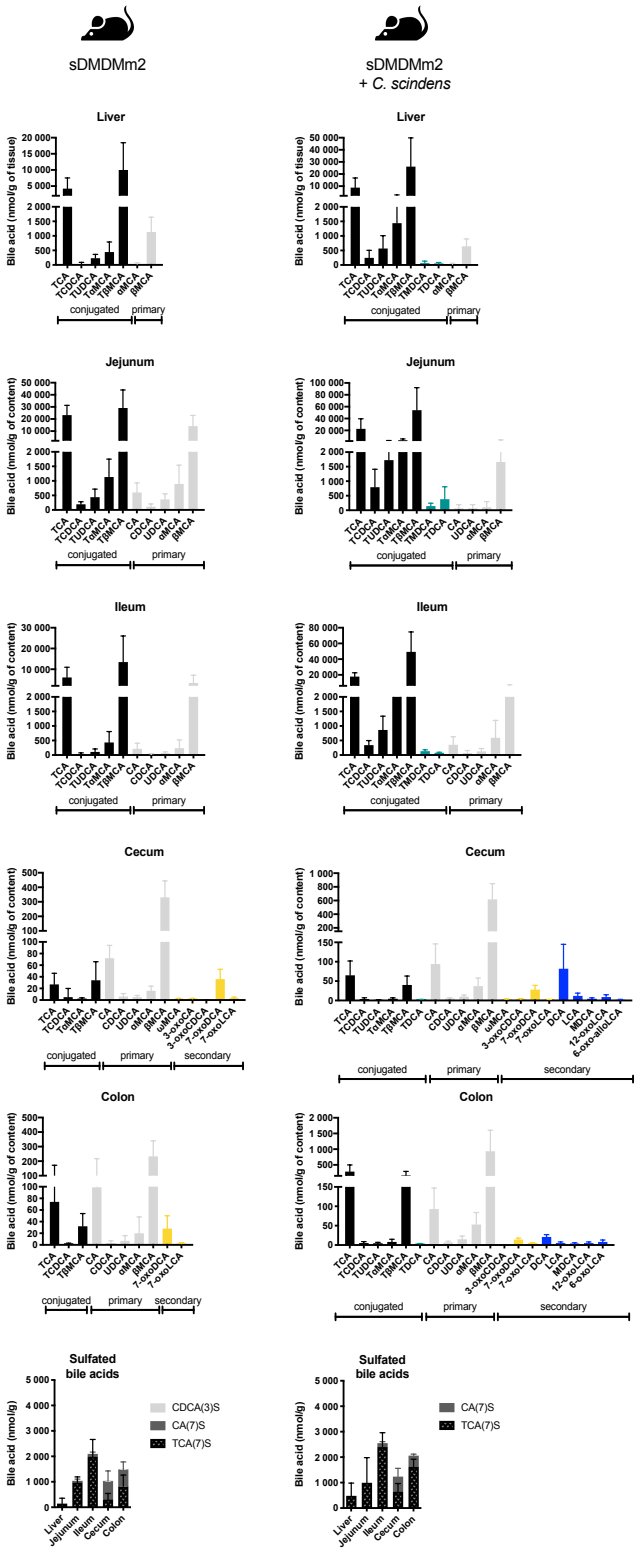

Figure 2 | Bile acid composition along the intestinal tract of sDMDMm2 and *C. scindens*-colonized sDMDMm2 gnotobiotic mice based on LC-MS/MS analysis. sDMDMm2 mice (n=5)

and sDMDMm2 mice pre-colonized 7 days with *C. scindens* (n=5) were sacrificed and intestinal content samples were harvested and processed for bile acid LC-MS/MS measurements. Values indicate measured bile acid concentrations in nmol/g of tissue or intestinal content. Black bars indicate primary conjugated bile acids, teal bars secondary conjugated BAs, gray bars primary deconjugated BAs, yellow bars secondary BAs (all but 7-dehydroxylated), and blue bars represent 7-dehydroxylated BAs.

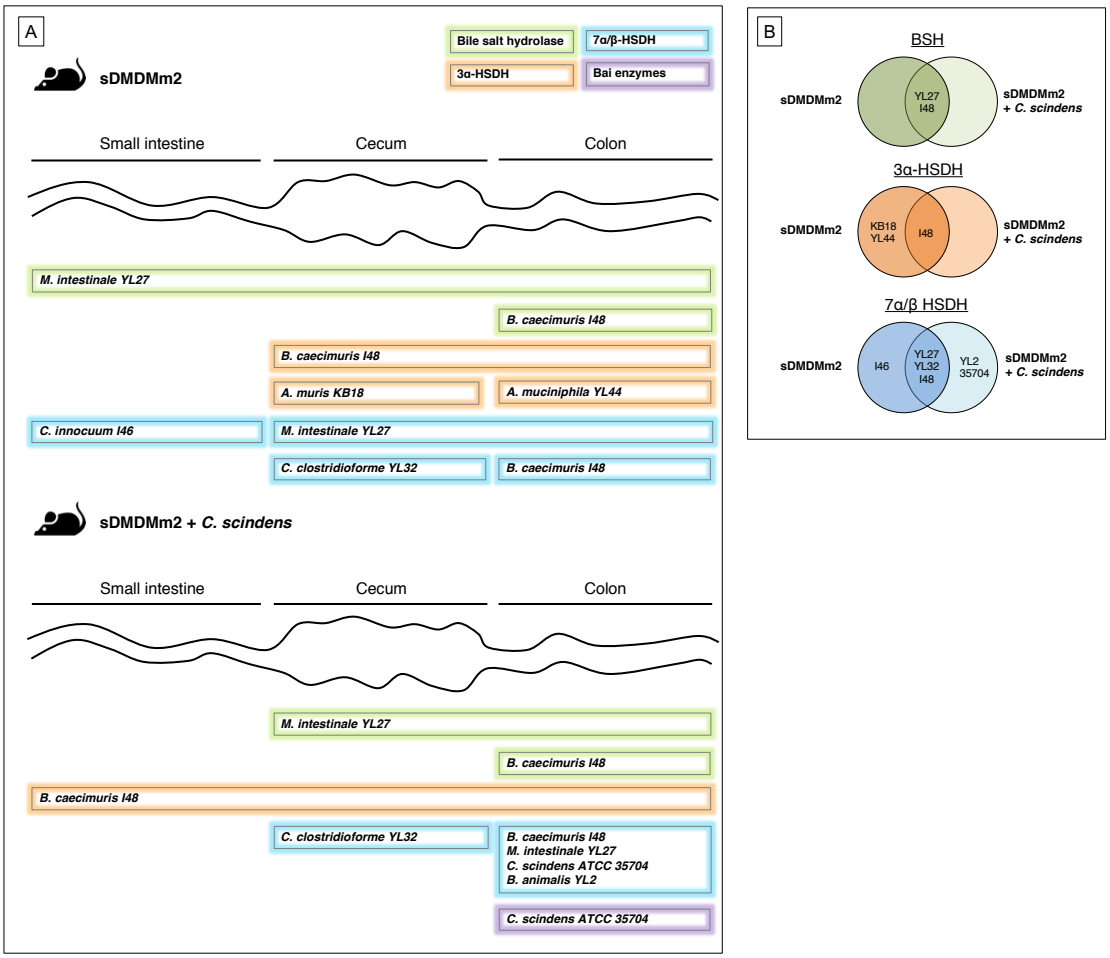

Figure 3 | Biogeography of specific bile-acid transformation enzymes and the associated microorganisms based on metaproteomic analysis.

sDMDMm2 mice (n=3) and sDMDMm2 mice pre-colonized 7 days with *C. scindens* (n=3) were sacrificed and intestinal content samples were harvested and processed for metaproteomic analysis. Metaproteomes were mined to find homologous sequences of known bile salt hydrolases (BSH), 3α/β-HSDH, 7α/β-HSDH and 12α-HSDH as well as *C. scindens bai* genes. A) Scheme illustrating where bile salt hydrolases, 3α-, 7α- and 7β-hydroxysteroid dehydrogenase (HSDH) and Bai enzymes are expressed in the gut and which are the bacterial species producing these enzymes. 12α-HSDH and 3β-HSDH were not detected in the metaproteome, and therefore are not presented on this figure. Almost all enzymes indicated on panel A were found in the three biological

triplicates (Table S8). The only one that was found in only 2 mice out of 3 is the 3α-HSDH from *B. caecimuris I48* in the small intestine (Table S8). B) Venn diagrams summarizing the bile acid -metabolizing enzymes detected in sDMDMm2 mice and *C. scindens*-colonized sDMDMm2 mice metaproteomes. For each enzyme detected, the strain producing the enzyme is indicated on the diagram, on the left or right circle if the enzyme was detected in sDMDMm2 mice or *C. scindens*-colonized sDMDMm2, respectively. If an enzyme was found in both sDMDMm2 and *C. scindens* colonized-sDMDMm2 mice, the producing-strain is indicated in the overlapping part of the two circles.

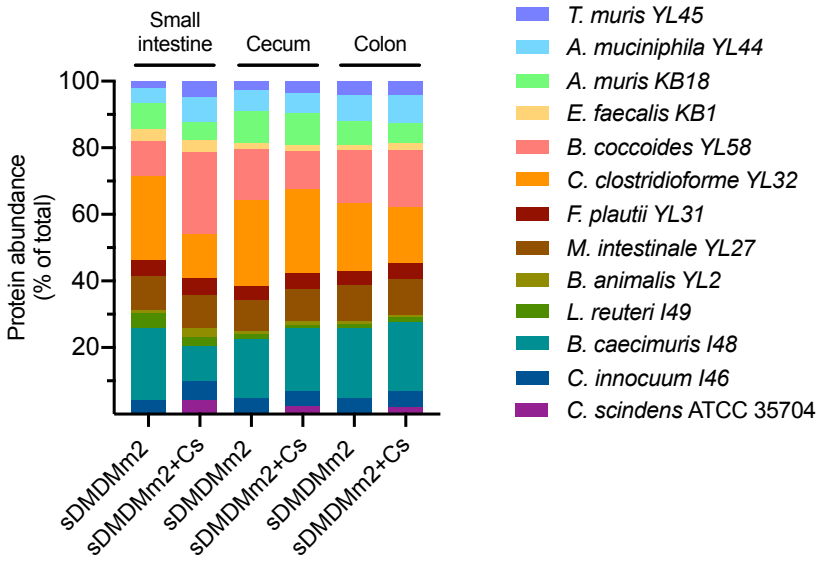

Figure 4 | Protein abundance along the intestinal tract of sDMDMm2 and *C. scindens*-colonized sDMDMm2 gnotobiotic mice based on the metaproteomic analysis of intestinal content. sDMDMm2 mice (n=3) and sDMDMm2 mice pre-colonized 7 days with *C. scindens* (n=3) were sacrificed and intestinal content samples were harvested and processed for metaproteomic analysis. Of note, proteins (2-4% of total) in the control mice were assigned to *C. scindens* ATCC 35704 and are not depicted in this figure. Contamination of control mice with *C. scindens* was evaluated experimentally by plating and confirmed to be negative. *C. scindens* protein misassignment is likely due to genome

ASBMB JOURNAL OF LIPID RESEARCH

relatedness, which is a current challenge in the field of metaproteomic. Using a more stringent approach (matched metaproteome database), we resolved this issue of genome relatedness and did not detect *C. scindens* proteins in control mice (Figure S3).

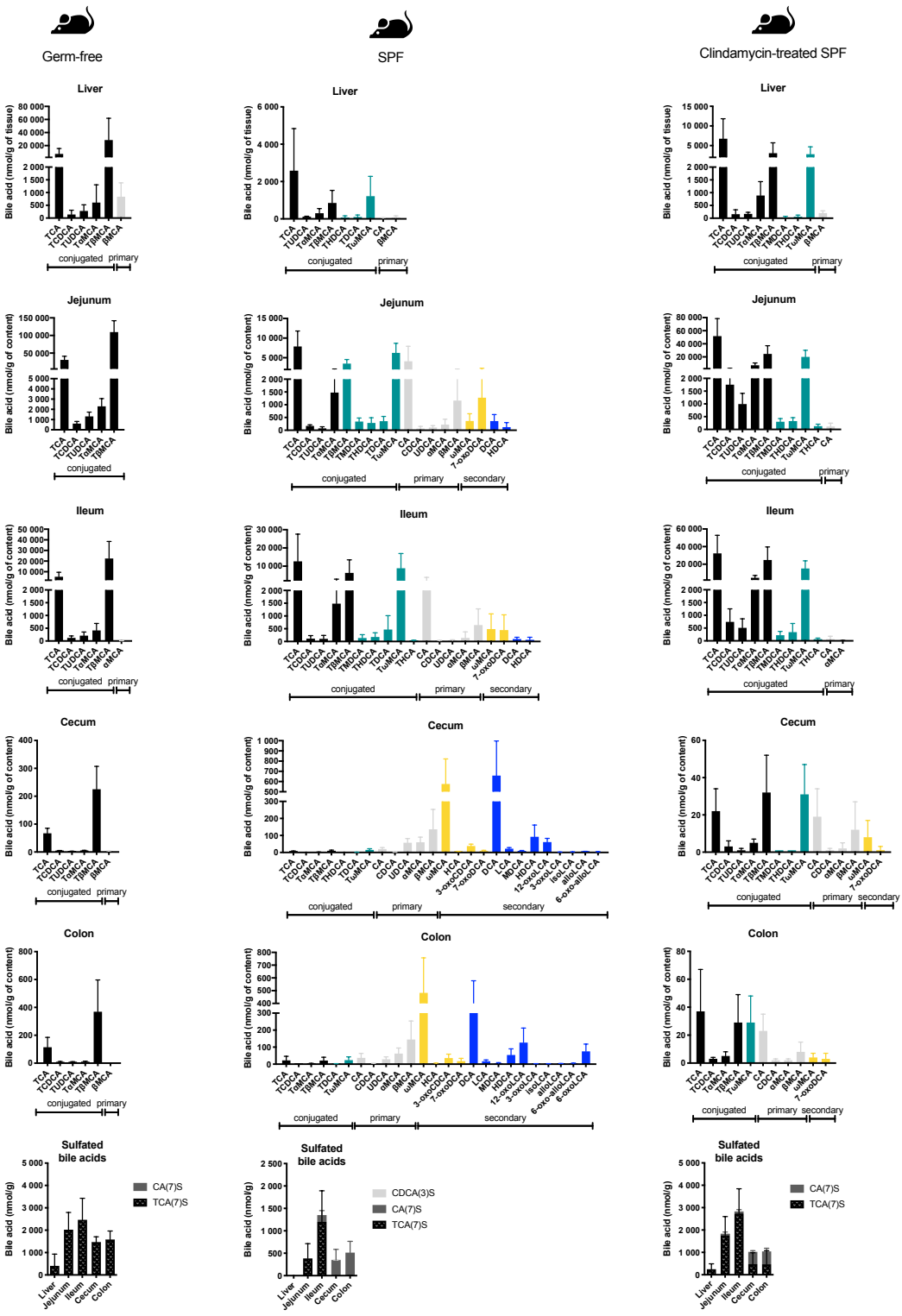

Figure 5 | Bile acid composition along the intestinal tract in germ-free, SPF, and clindamycin-

treated SPF mice based on LC-MS/MS analysis. SPF mice were pre-treated with clindamycin 24h before sacrifice. Intestinal content samples were harvested from GF mice (n=5), SPF mice (n=5), clindamycin-treated SPF mice (n=5). Samples were processed for bile acid LC-MS/MS measurements. Values indicate measured bile acid concentrations in nmol / g of tissue or intestinal content. Black bars indicate primary conjugated bile acids, teal bars secondary conjugated BAs, gray bars primary deconjugated BAs, yellow bars secondary BAs (all but 7-dehydroxylated), and blue bars represent 7-dehydroxylated BAs.

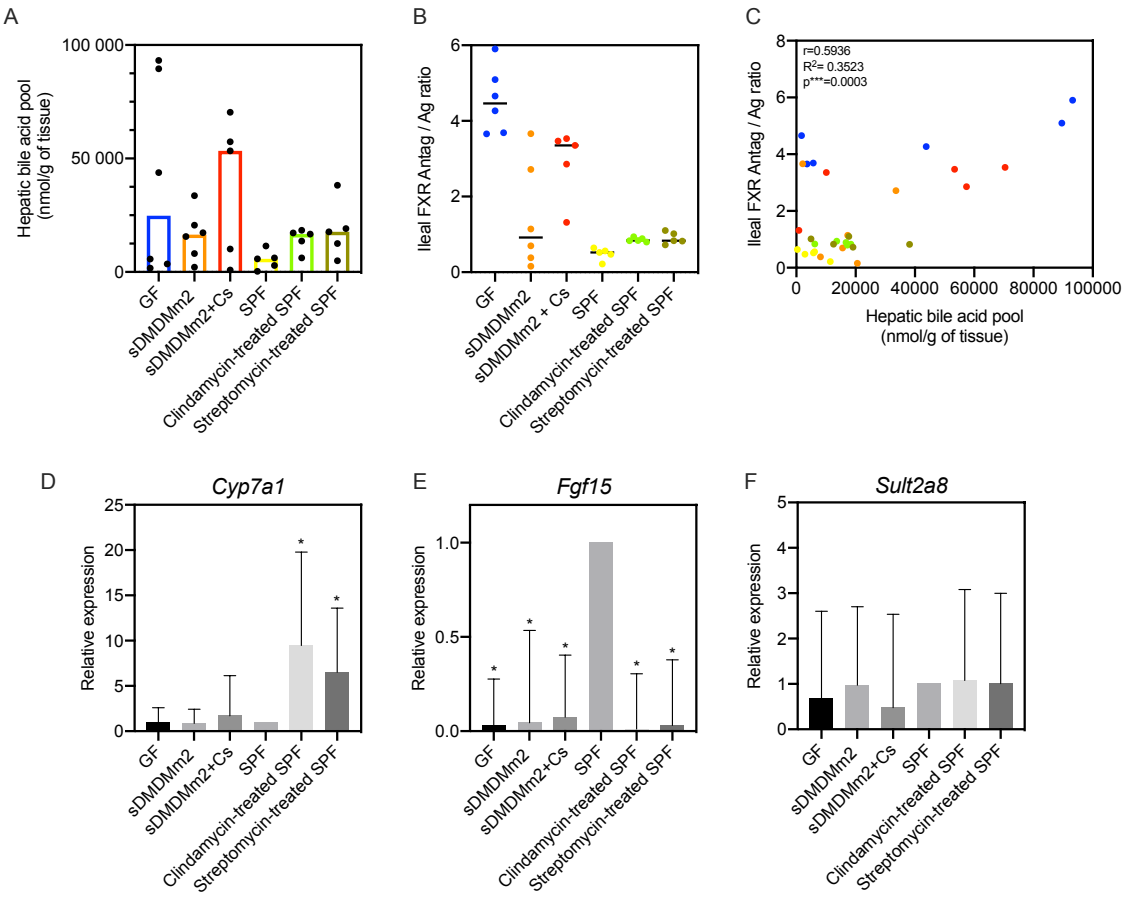

Figure 6 | Probing the influence of the gut microbiota on BA synthesis and detoxification. A) Hepatic bile acid pool. Each dot corresponds to an individual mouse. Histograms show the median of the hepatic bile acid pool for the mouse models considered. B) ileal FXR antagonist/agonist ratio. TαMCA, TβMCA were considered to be FXR antagonists and CDCA, CA, DCA, LCA, TCDCA, TCA, TDCA and TLCA, FXR agonists according to Parks *et al.* (1999)[59]. Each dot corresponds to an individual mouse. The horizontal bar in the scatter dot plot indicates the median for the mouse models considered. C) Correlation between the hepatic bile acid pool and the ileal FXR antagonist/agonist ratio. Each dot corresponds to an individual mouse. Pearson correlation analysis was computed with GraphPad Prism. D, E, F) Gene expression of *Cyp7a1, Fgf15* and *Sult2a8* in each mouse model considered relative to SPF mice (n=5 mice for each mouse model). A value of 1 is attributed to SPF mice. * indicates a p-value < 0.05.